https://doi.org/10.5194/acp-2020-312
Preprint. Discussion started: 26 May 2020

Atmospheric Chemistry and Physics
Discussions

A set of methods to quantitatively evaluate the below-cloud evaporation effect on precipitation isotopic composition: a case study in a city located in the semi-arid regions of Chinese Loess Plateau

Meng Xing[1,2*], Weiguo Liu[1,2,3*], Jing Hu[1,2]

1.State Key Laboratory of Loess and Quaternary Geology, Institute of Earth Environment, Chinese Academy of Sciences, Xi’an, 710061, China

2.CAS Center for Excellence in Quaternary Science and Global Change， Xi'an, 710061, China.

3. University of Chinese Academy of Sciences, Beijing, 100049, China

Corresponding authors:

Meng Xing email address: xingmeng@ieecas.cn

Weiguo Liu email address: liuwg@loess.llqg.ac.cn

https://doi.org/10.5194/acp-2020-312
Preprint. Discussion started: 26 May 2020

Atmospheric Chemistry and Physics Discussions
Open Access
EGU

Abstract:

Below-cloud evaporation effect heavily alters the initial precipitation isotopic composition, especially in the arid and semi-arid regions, and leads to misinterpreting the isotopic signal. To correctly explore the information contained in the precipitation isotopes, the first step is to qualitatively analyze the falling raindrops encountered below-cloud processes, and then to quantitatively compute the below-cloud evaporation ratio of raindrops. Here, based on two-year precipitation and water vapor isotopic observations in Xi'an, we systematically evaluated the variations of precipitation and water vapor isotopes caused by the below-cloud evaporation effect. Our results suggest that the equilibrium method could be successfully used to predict the ground-level water vapor isotopic composition in semi-arid climates, especially for the winter data. Moreover, by using △d△δ-diagram, our data showed that evaporation is the mainly happened below-cloud process of raindrops, while snowfall samples retained the initial cloud signal because of less isotopic exchange between vapor and solid phases. In terms of meteorological factors, both temperature, relative humidity, and precipitation amount affect the intensity of below-cloud evaporation. In arid and semi-arid regions, the below-cloud evaporation ratio computed by the mass conservation equation would be overestimated relative to the isotopic method, while relative humidity is the most sensitive parameter in computing the remaining fraction of evaporation. In the Chinese Loess Plateau (CLP) city, raindrops are weakly evaporated in autumn and winter, and heavily evaporated in spring and summer, and in the meantime, the evaporation intensity is related to the local relative humidity. Our work sets an integrated and effective method to evaluate the below-cloud evaporation effect, and it will improve our understanding of the information contained in precipitation isotopic signals.

https://doi.org/10.5194/acp-2020-312
Preprint. Discussion started: 26 May 2020

Atmospheric Chemistry and Physics Discussions

1 Introduction

Hydrogen and oxygen isotopes of precipitation are the one of greatly important tools to trace the hydrological cycle and climate changes (Bowen et al., 2019; Gat, 1996). For the paleoenvironment, the isotopic signals of precipitation recorded in ice cores (Thompson et al., 2000; Yao et al., 1996), tree rings (Liu et al., 2004; Liu et al., 2017b), speleothems (Cai et al., 2010; Tan et al., 2014), and leaf wax of loess-paleosol deposits (Wang et al., 2018b) and lake sediments (Liu et al., 2017a, 2019) could be used to reconstruct the information of temperature, precipitation, and hydrological regimes in geologic history, as it had participated into the formation or growth of these geological archives. For the modern environment, the isotopic ratios of precipitation could be used to quantitatively constraint the water vapor contribution from advection (Peng et al., 2011), evaporation (Sun et al., 2020; Wang et al., 2016a), transpiration (Li et al., 2016a; Zhao et al., 2019), and even anthropogenic activities (Fiorella et al., 2018; Gorski et al., 2015), as precipitation itself is one of the most important parts of the water circulation processes. Due to the limitations from sampling and theory, however, there remains some uncertainty to decipher the information contained in precipitation by using hydrogen and oxygen isotopic ratios (Bowen et al., 2019; Yao et al., 2013).

Chinese Loess Plateau (CLP) is located in the arid and semi-arid areas, where the below-cloud evaporation and surface moisture evaporation effects on precipitation isotopes have been widely proved (Sun et al., 2020; Wan et al., 2018; Zhang and Wang, 2016)， which means the information remained in precipitation isotopic composition may have been remodeled by the environmental factors. Therefore, before we utilize precipitation isotopes to reconstruct the climate changes or to trace the water vapor sources, we first need to have a set of reliable evaluation systems to diagnose whether the precipitation isotopic ratios have been distorted by the below-cloud evaporation effect. Second, we should quantitatively calculate the below-cloud evaporation ratio of precipitation. Lastly, we can be able to use the calibrated precipitation isotopes to discuss regional water vapor sources or global hydrological cycle after we exclude the below-cloud evaporation effect. But the present situation is that there is still a large gap in our understanding at the first and second steps, and hence further study is needed.

Over the past decades, to determine whether the hydrometeors have been evaporated during its falling, most studies depend on a second-order isotopic parameter (Jeelani et al., 2018; Li and Garzione, 2017), deuterium excess (defined as d-excess= δ^2H-

https://doi.org/10.5194/acp-2020-312
Preprint. Discussion started: 26 May 2020

$8\times\delta^{18}O$), which is the representative of the kinetic fractionations, since $^{2}H^{1}H^{16}O$ equilibrate faster than $^{1}H_2{}^{18}O$ in different phases (Clark and Fritz, 1997; Dansgaard, 1964). The lighter isotopes (^{1}H and ^{16}O) of raindrop are preferentially evaporated from the liquid phase during its falling through unsaturated ambient air, which results in a decrease of d-excess in rain. Accordingly, the d-excess in the surrounding water vapor will increase. The slope of the local meteoric water line (LMWL) has also been widely used as a metric to infer the below-cloud evaporation effect according to the theory of water isotopic equilibrium fractionation (Chakraborty et al., 2016; Putman et al., 2019; Wang et al., 2018a), in which the LMWL's slopes approximately equal to 8.0 belonging to equilibrium fractionation and that is lower than 8.0 pointing to a non-equilibrium fractionation, such as the re-evaporation of raindrops. Nonetheless, it should be noted that a change of air masses, condensation in supersaturation conditions, and moisture exchange in the cloud and sub-cloud layer also cause largely spatial variation in slopes and d-excess values (Graf et al., 2019; Putman et al., 2019; Tian et al., 2018). As an improvement, simultaneous observations of water vapor and precipitation are applied to distinguish these processes and quantify below-cloud processes. Yu et al. (2015, 2016) used the custom-made sampling devices to collect daily water vapor samples over the Tibetan and Pamir Plateau, and discussed moisture source impacts on the precipitation isotopes. With the aid of the off-line water vapor sampling system, Deshpande et al. (2010) analyzed the rain-vapor interaction using stable isotopes. However, the old water vapor cryogenic trapping technique is time-consuming (Christner et al., 2018), labor-intensive (Welp et al., 2012), and discrete (Wen et al., 2016), limiting the further examination of the two-phase system.

In recent years, with the progress in optical laser systems, the relatively portable field-deployable laser spectroscopic instruments, simultaneously measuring $^{1}H_2{}^{16}O$, $^{2}H^{1}H^{16}O$, and $^{1}H_2{}^{18}O$ isotopes, allows performing online, autonomous, and long-term site measurements of the water vapor stable isotopic composition (Aemisegger et al., 2012; Christner et al., 2018). The emergence of this instrument exerts a great impact on the study of water vapor isotopic composition, leading to a substantially increased number of observations in near-ground water vapor, and deepens our knowledge in water vapor isotopic variations and fractionation processes during the two-phase transformation (Noone et al., 2011; Steen-Larsen et al., 2014). Wen et al. (2010) first analyzed the d-$excess_{vap}$ (denotes the d-excess of water vapor) at hourly temporal resolution in Beijing, China, and systematically discussed the controls on the isotopic exchange between vapor and condensed phase. Griffis et al. (2016) used multi-years

https://doi.org/10.5194/acp-2020-312
Preprint. Discussion started: 26 May 2020

Atmospheric Chemistry and Physics Discussions

water vapor and precipitation isotopic results to evaluate the water vapor contributions to the planetary boundary layer from evaporation. Laskar et al. (2014) and Rangarajan et al. (2017) comprehensively investigated the water vapor sources and raindrop-vapor interaction in Taibei, and developed a box model to explain the controlling factors for high and low d-excess$_{vap}$ events in this region. Combined with observations and numerical simulations of stable isotopes in vapor and rain impacted by cold fronts, Aemisegger et al. (2015) clearly revealed the importance of below-cloud processes for improving the simulations. As a creative work, Graf et al. (2019) introduced a new interpretive framework to directly separate the convoluted influences on the stable isotopic composition of vapor and precipitation according to the theoretical fractionation processes, especially the influences of equilibration and below-cloud evaporation, which enables us to correctly figure out the governing below-cloud processes in the course of a rainfall. Although Graf's et al. (2019) work gives us a new guideline to more accurately judge the raindrops experienced below-cloud evaporation effect, their work was only validated on a cold frontal rain event of short period, and hence more works should be done to prove the general applicability of their framework.

On the other hand, to quantitatively calculate the below-cloud evaporation ratio of raindrops, the falling raindrop model suggested by Stewart (1975) has been widely used, as the raindrops experienced physical processes have been explicitly described by this isotope-evaporation model (Müller et al., 2017; Sun et al., 2020; Zhao et al., 2019). Based on Stewart's (1975) work, the remaining fraction of raindrop mass (F_r) after evaporation could be calculated according to the difference of stable isotopic ratios in collected precipitation near the ground and below the cloud base (See Data and Methods, section 2.3.2, eq 7). We note that some of the studies used the mass conservation model of a falling raindrop to calculate F_r (See Data and Methods, section 2.3.3, eq 8; Kong et al., 2013; Li et al., 2016; Sun et al., 2019; Wang et al., 2016b), and some of the works assumed the F_r is a constant (Müller et al., 2017), but no work has been reported by using ground-based and cloud-based observations of water vapor isotopes to calculate the F_r according to our knowledge. Due to the numerous uncertainty of the parameters in the mass conservation model, such as the factors of terminal velocity, the evaporation intensity, and the diameter of the raindrops, the error propagation will largely raise the deviation of F_r in the model. Furthermore, no work has systematically evaluated the differences of F_r computed by the observed isotope results and the classical mass conservation model, until now.

https://doi.org/10.5194/acp-2020-312
Preprint. Discussion started: 26 May 2020

Here, we have measured the near-ground water vapor isotopic composition at a city located in the CLP for 2 years, while collected 142 precipitation samples (including snowfall samples). The objectives of this study are to: 1. test the applicability of the △d△δ-diagram suggested by Graf et al. (2019) when it is used to diagnose the below-cloud processes; 2. compare the differences of raindrops below-cloud evaporation ratio calculated by the observed ground-based water vapor isotopic composition and the mass conservation model; 3. understand the main meteorological factors, such as temperature, relative humidity (RH), and precipitation amount, controlling on the below-cloud evaporation effect, and the seasonal variations of below-cloud evaporation ratio in CLP. With the advantages of the coupling observations of the vapor and precipitation in stable isotopes near the ground level, this study will provide a new set of methods to determine the below-cloud evaporation effect qualitatively, and strengthen our insight into that effect in arid and semi-arid areas quantitatively.

2 Data and methods

2.1 Sampling site

As the capital city of Shaanxi province and the largest city in northwest China, Xi'an is located on the Guanzhong Plain on the southern edge of the CLP at an average elevation of 400 m. The city is located in a semi-arid to arid region and is representative of most cities in the north and northwest of China (e.g., Lanzhou and Xining city, Fig. 1), while notable below-cloud evaporation effect has been reported by many studies in this area (Sun et al., 2020; Wan et al., 2018; Zhu et al., 2016).

https://doi.org/10.5194/acp-2020-312
Preprint. Discussion started: 26 May 2020

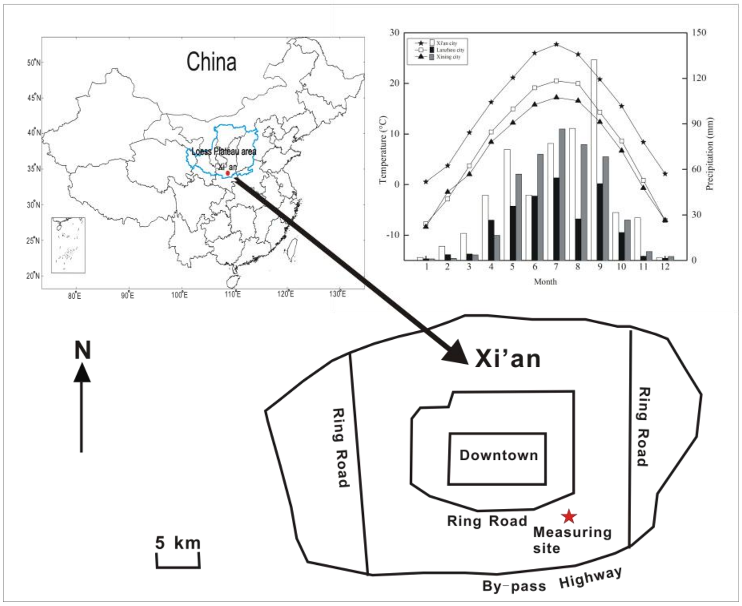

Figure 1 Average monthly variations of temperature and precipitation in Xi’an, Lanzhou, and Xining during 2010-2015. Location of the sampling site in the Yanta Zone, 9 km SE of downtown Xi’an. Water vapor samples are taken on the seventh floor of a twelve-story building, about 30 m above ground level. Precipitation samples are collected on the top floor, 1 m above ground level.

The water vapor in-situ measurement is located in a residential area, approximately 10 km southeast to downtown of Xi’an city (Fig. 1). No specific pollution sources or point sources are adjacent to the site. The atmospheric water vapor isotopic composition was observed from 1 January 2016 to 31 December 2017 on the seventh floor of the Institute of Earth and Environment, Chinese Academy of Sciences, about 30 m above ground level. The rainfall or snowfall collector was placed on the rooftop of the buildings (1 m above the floor of the roof).

2.2 Sampling and isotopic measurement

Rainfall and snowfall samples were collected manually from the beginning of each precipitation event using a polyethylene collector (700 mm × 450 mm × 170 mm) and the volume was measured using a graduated flask. Before being used, the collector was cleaned with soap and water, rinsed with deionized water, and then dried. When the precipitation events end, the collector was quickly taken back to minimize water evaporation. Rainfall samples were immediately poured into a 100 ml polyethylene bottle. The snowfall samples were melted at room temperature in a closed plastic bag after collection, and then immediately poured into a 100 ml polyethylene bottle. After

https://doi.org/10.5194/acp-2020-312
Preprint. Discussion started: 26 May 2020

collection, samples were filtered through 0.40–μm polycarbonate membranes. About a 2 ml of each filtrate was transferred into a sample vial, and stored at – 4°C until being measured. Of the 142 samples, during the two-year sampling campaign, we collected 131 rainfall and 11 snowfall samples (Table S1).

In all cases, the data are reported in the standard delta notation (δ), i.e., the per mil (‰) deviation from Vienna Standard Mean Ocean Water according to, δ= (R_{sample}/$R_{reference}$-1) ×1000, where R is the isotope ratio of the heavy and light isotope (e.g., $^{18}O/^{16}O$) in the sample and the reference.

The precipitation samples were measured by Picarro L2130-i wavelength-scanned cavity ring-down spectrometer at high-precision model, with the precision of better than 0.1‰ and 0.5‰ for $\delta^{18}O$ and $\delta^{2}H$, respectively (Crosson, 2008; Gupta et al., 2009). All the samples were calibrated by three laboratory standards, while the $\delta^{18}O$ and $\delta^{2}H$ true values of the three laboratory standards (Laboratory Standard-1 (LS-1): $\delta^{18}O$ =+0.3‰, $\delta^{2}H$ =–0.4‰; Laboratory Standard-2 (LS-2): $\delta^{18}O$ =–8.8‰, $\delta^{2}H$ =–64.8‰; Laboratory Standard-3 (LS-3): $\delta^{18}O$ =–24.5‰, $\delta^{2}H$ =–189.1‰) are calibrated to the scale of two international standard material VSMOW-GISP.

Atmospheric water vapor $\delta^{18}O_v$ and $\delta^{2}H_v$ were also measured by Picarro L2130-i, but at a liquid-vapor dual model. The inlet of the gas-phase instrument is connected to the vapor source through an external solenoid valve when measuring vapor samples. This valve can switch the input of the instrument from the vapor sample to dry gas. The instrument is connected to dry gas prior to being connected to the evaporator for measuring liquid water standards so that any traces of the water vapor sample are removed from the measurement cell. The standards are injected into the evaporator and measured by a CTC Analytics autosampler, PAL HTC-xt (Leap Technologies, Carrboro, NC, USA). The atmospheric water vapor is pumped through a stainless-steel tube (1/8 inch) using a diaphragm pump and detected by the laser spectrometer.

The raw water vapor $\delta^{18}O_v$ and $\delta^{2}H_v$ data were obtained approximately at 1 Hz and then block-averaged into 24 h intervals. As the main usage of this instrument is to measure the liquid water samples in our laboratory, it is used to monitor the water vapor isotopes in its spare time. Thus, the data gaps represent the instrument is in liquid samples measuring status or maintenance.

https://doi.org/10.5194/acp-2020-312
Preprint. Discussion started: 26 May 2020

The hourly meteorological data, such as temperature and RH in Xi'an, are reported by the China meteorological administration, and can be downloaded from the websites of http://www.weather.com.cn/. The meteorological station is about 10 km to the north of our sampling site.

2.3 Water vapor isotopic data calibration

Due to the isotopic measurements of the cavity ringdown spectrometer with water vapor concentration effect as outlined by some studies (Bastrikov et al., 2014; Benetti et al., 2014; Steen-Larsen et al., 2013), it is important to determine the humidity-isotope calibration response function. Because we did not have the Standards Delivery Module (Picarro) system or equivalent, the humidity calibration is based on data obtained from discrete injections of three known liquid standards with a PAL autosampler and the Picarro vaporizer unit (Benetti et al., 2014; Noone et al., 2013). The analyzer is programmed to perform a self-calibration after every 24 hours of ambient air measurement using an autosampler to inject liquid standards for producing different humidity. Injections were arranged at humidity levels near 3000, 5000, 8000, 10000, 15000, 20000, 25000 and 30000 ppm. Each reference sample is measured continuously for 8 times at one humidity level, and the last 3 times results were used to calculate the average to be recognized as the δ-value at the measured humidity. The humidity correction is the difference between the δ-value at the measurement humidity and the δ-value at a reference value taken as humidity = 20000 ppm. The best fit was reached with an exponential function for $\delta^{18}O_v$ and a linear function for δ^2H_v (Fig. S1a and S1b). The isotopic measurements of ambient air $\delta^{18}O_v$ samples were corrected for humidity effects using:

$$\delta^{18}O_{\text{humidity calibration}} = \delta^{18}O_{\text{measured}} - (-4.91 \times e^{(-3.51 \times \text{Measured humidity})}) \quad \text{(eq 1)}$$

and for ambient air δ^2H_v humidity correction using:

$$\delta^2H_{\text{humidity calibration}} = \delta^2H_{\text{measured}} - (0.0001\times \text{Measured humidity} - 1.86) \quad \text{(eq 2)}$$

where $\delta_{\text{humidity calibration}}$ is the calibrated data for water vapor stable isotope; δ_{measured} is the raw, measured data before calibration; and measured humidity is the corresponding humidity at the time of measurement.

2.4 Analytical methods

2.3.1 △d△δ-diagram

As the raindrop falling from the cloud base to the ground, part of it will be evaporated into the ambient atmosphere, however, it is very hard to quantify this process by observation. Using stable water isotopes, Graf et al. (2019) introduced a △d△δ-

https://doi.org/10.5194/acp-2020-312
Preprint. Discussion started: 26 May 2020

diagram to diagnose below-cloud processes and their effects on the isotopic composition of vapor and rain since equilibration and evaporation are two various below-cloud processes and lead to different directions in the two-dimensional phase space of the △d△δ-diagram. Here, the differences of isotopic composition ($\delta^{18}O_{pv\text{-}eq}$, d-$excess_{pv\text{-}eq}$) of equilibrium vapor from precipitation samples relative to the observed ground-based water vapor ($\delta^{18}O_{gr\text{-}v}$, d-$excess_{gr\text{-}v}$) can be expressed as:

$$\Delta\delta=\delta_{pv\text{-}eq}-\delta_{gr\text{-}v} \qquad \text{(eq3)}$$

$$\Delta \text{d-excess}_{v}=\text{d-excess}_{pv\text{-}eq}-\text{d-excess}_{gr\text{-}v} \qquad \text{(eq4)}$$

where $\delta_{pv\text{-}eq}$ and $\delta_{gr\text{-}v}$ are the $\delta^{2}H$ ($\delta^{18}O$) of water vapor below the cloud base and near the ground, respectively, and d-$excess_{pv\text{-}eq}$ and d-$excess_{pv\text{-}eq}$ are d-excess values of water vapor below the cloud base and near the ground, respectively.

To calculate the water vapor isotopic composition below the cloud base, we hypothesize the constant exchange of water molecules between the liquid the vapor phases during the falling of raindrop, and the isotopic compositions reach towards an equilibrium in the two phases during the processes. In the equilibrium state, the isotopic fractionation between the liquid and vapor phases follows a temperature-dependent factor:

$$R_{p}=R_{pv\text{-}eq}\alpha \qquad \text{(eq5)}$$

where $R_{pv\text{-}eq}$ is the water vapor isotope ratio between heavy and light isotopes ($^{2}H/^{1}H$ and $^{18}O/^{16}O$), R_p is the isotope ratio in precipitation, and α is a temperature-dependent equilibrium fractionation factor. Here, when the temperature is greater than 0 °C, we use the equation of Horita and Wesolowski (1994) to calculate $^{2}\alpha$ and $^{18}\alpha$, when the temperature is below 0 °C, the equilibrium fractionation factor suggested by Ellehoj et al. (2013) is considered.

The above equation can be converted into δ-notation as:

$$\frac{\delta_p}{1000}+1=\alpha\left(\frac{\delta_{pv\text{-}eq}}{1000}+1\right) \qquad \text{(eq6)}$$

where δ_p is the isotope ratio in precipitation.

2.3.2 Below-cloud evaporation calculated by isotope

Stewart (1975) suggested the falling raindrop isotopic fractionation of evaporation could be calculated according to the fraction of raindrop mass remained after evaporation:

https://doi.org/10.5194/acp-2020-312
Preprint. Discussion started: 26 May 2020

$$\Delta\delta=\delta_p-\delta_{zp\text{-}eq}=(1-\frac{\gamma}{\alpha})(F_{iso}^{\beta}-1) \quad \text{(eq7)}$$

where δ_p and $\delta_{zp\text{-}eq}$ are precipitation isotope ratio near the ground and below the cloud base, respectively; F_{iso} is the remaining fraction of raindrop mass after evaporation (hereafter, the remaining fraction of raindrop mass calculated by this method is denoted as F_{iso}); α is equilibrium fractionation factor for hydrogen and oxygen isotopes; the parameters of γ and β is defined by Stewart (1975). For the detailed calculation processes, please refer to the supplemental material (Appendix A), and Wang et al. (2016b), Sun et al. (2020), and Salamalikis (2016).

2.3.3 Below-cloud evaporation calculated by mass conservation model

Before the advent of the laser-based spectrometer, the method, which calculates the remaining fraction of raindrop mass according to the law of conservation of mass (hereafter, the remaining fraction of raindrop mass calculated by this method is denoted as $F_{raindrop}$), has been widely used (Kong et al., 2013; Li et al., 2016a; Sun et al., 2020; Wang et al., 2016b; Zhao et al., 2019):

$$F_{raindrop}=\frac{m_{end}}{m_{end}+m_{ev}} \quad \text{(eq8)}$$

where the mass of the reaching ground raindrop without evaporation is m_{end} and the evaporated raindrop mass is m_{ev}. For the detailed calculation processes, please refer to the supplemental material (Appendix B), and Wang et al. (2016b), Sun et al. (2020), Kong et al. (2013), and Salamalikis (2016).

2.3.4 Statistical Analysis

To compare the difference of the below-cloud evaporation calculated by the two methods, the independent t-test was performed on SPSS 13.0 (SPSS Inc., Chicago, US). A significant statistical difference was set at $p < 0.05$.

3 Results and discussion

3.1 Relationship between water vapor and precipitation isotope ratios

In this study, the local meteoric water line (LMWL) is: $\delta^2H_p=7.0\times\delta^{18}O_p+3.0$ based on event-based precipitation isotopic composition, and the local water vapor line (LWVL) is: $\delta^2H_v=7.6\times\delta^{18}O_v+10.0$ based on daily water vapor isotopic composition (Fig. 2). Both the slope and intercept of LMWL are lower than that of Global Meteoric Water Line (GMWL), which are 8.0 and 10.0 (Dansgaard, 1964; Gat, 1996), respectively, indicating the potential for significant below-cloud evaporation effect on precipitation (Froehlich et al., 2008). In general, the slope of the meteoric water lines are indicative

https://doi.org/10.5194/acp-2020-312
Preprint. Discussion started: 26 May 2020

Atmospheric Chemistry and Physics Discussions

of kinetic processes superimposed on the equilibrium fractionation, and the slope of LWVL (slope=7.6) that shows a little lower than that of expected equilibrium fractionation (slope=8.0) is also associated with the increasing influence of kinetic processes (Rangarajan et al., 2017).

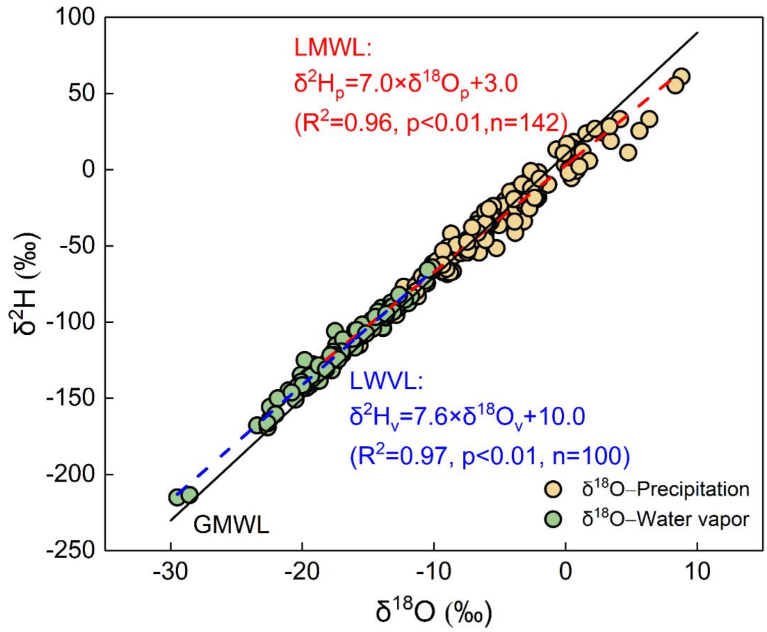

Figure 2 Local meteoric water line (LMWL) and Local water vapor line (LMVL) in Xi'an

Besides, we noted that the water vapor and precipitation isotopic composition basically followed the same trend, and the water vapor isotopic composition is roughly more negative than the precipitation isotopic composition (Fig. 2). According to the classical isotopic fractionation theory, the heavier isotopes preferentially condense into the liquid phase, and results in the precipitation isotopic ratios being more positive than the corresponding water vapor isotopic composition during the precipitation process (Dansgaard, 1964). Hence, the perfect distribution characteristics of water vapor and precipitation on the $\delta^{18}O$-$\delta^{2}H$ plot would make us suppose that the precipitation isotopic composition is mainly determined by its local water vapor isotopic composition in this study site. To further validate our assumption, each of the event-based precipitation isotopic ratio was plotted together with its water vapor isotopic composition of the corresponding day, and they showed a significant positive correlation (Fig. 3a, R^2=0.66, p<0.01). The water vapor isotopic composition can explain above 60% of the variation of precipitation isotopic composition. Further, we used the measured precipitation isotopic composition to deduce the water vapor isotopic composition at the cloud base

https://doi.org/10.5194/acp-2020-312
Preprint. Discussion started: 26 May 2020

Atmospheric Chemistry and Physics Discussions

(1500m) according to the liquid-vapor equilibrium isotope fractionation, and compared it with the observed near-ground water vapor isotopic composition. As expected, the scatterplot of the observed $\delta^{18}O_v$ against the deduced $\delta^{18}O_{v\text{-}eq(1500m)}$ also presented a significantly positive relationship, and the correlation coefficient increased a little as well (Fig. 3b).

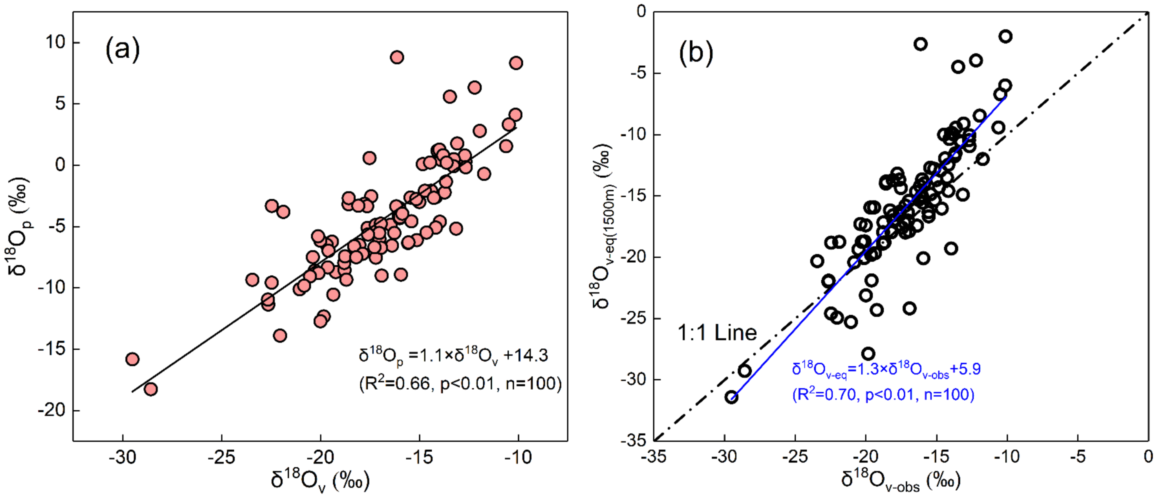

Figure 3 Relationship between $\delta^{18}O_p$ of precipitation and $\delta^{18}O_v$ of water vapor in Xian (a); and relationship between the equilibrium computed 1500m $\delta^{18}O_v$ based on the precipitation isotopic composition and the near ground observed $\delta^{18}O_v$ (b). The dash-dot line in (b) stands for the 1:1 line, and the blue line represents the regression line of the data.

The reasonable agreement of $\delta^{18}O$ between observed water vapor and equilibrium prediction has been reported by Jacob and Sonntag (1991), Welp et al. (2008), and Wen et al. (2010), however, they postulated the different relationship underlying the $\delta^{18}O_v$ and $\delta^{18}O_{pv\text{-}eq}$. Jacob and Sonntag (1991) suggested that the water vapor isotopic composition is possible to be deduced from the corresponding precipitation isotopic composition, but Wen et al. (2010) pointed that the equilibrium method cannot accurately predict the ground-level water vapor isotopic composition in arid and semiarid climates. Here, our results indicate that it is possible to derive the isotope composition of atmospheric water vapor based on that of the precipitation in the semi-arid area.

In addition, we also noted that the equilibrium calculated $\delta^{18}O_{v\text{-}eq(1500m)}$ is relatively more positive than the $\delta^{18}O_{v\text{-}obs}$ (Fig. 3b). Conventionally, the water vapor isotopic composition decreases with the increase of altitude because of the decreasing temperature (Deshpande et al., 2010; Salmon et al., 2019). However, due to the CLP

https://doi.org/10.5194/acp-2020-312
Preprint. Discussion started: 26 May 2020

belonging to the semi-arid area, the raindrops are largely potential to be evaporated in the unsaturated atmosphere during their falling as well as the $\delta^{18}O_p$ is subject to more positive than its actual value. Therefore, the positively equilibrated $\delta^{18}O_{v\text{-}eq(1500m)}$ is caused by the below-cloud evaporation effect, which makes the $\delta^{18}O_{v\text{-}eq}$-$\delta^{18}O_{v\text{-}obs}$ points deviate from the 1:1 line. This reminds us that although the isotopic composition of water vapor can be derived from the precipitation, the below-cloud evaporation effect on altering the precipitation isotopic composition should be carefully noticed in the arid and semi-arid area.

3.2 Below-cloud processes indicated by △d△δ-diagram

Traditionally, to qualitatively assess the below-cloud evaporation of raindrop, the value of d-excess$_p$ is a benchmark, as the isotopically kinetic fractionation will cause d-excess$_p$ deviate from 10‰, which is a theoretical value under vapor-liquid equilibrium fractionation (Gat, 1996). Normally, below-cloud evaporation will move d-excess$_p$ below 10‰, and in comparison, mixing with the recycled water vapor from surface evaporation and plant transpiration will bring d-excess$_p$ above 10‰ (Craig, 1961; Dansgaard, 1964). However, considering the kinetic fractionation processes of moisture transportation, the d-excess$_p$ information recorded in the collected precipitation has been modified, and thus this enhances the uncertainty to gauge the below-cloud evaporation process by solely using d-excess$_p$. Moreover, it is unable to discern other below-cloud processes only based on d-excess$_p$. In contrast, the △d and △δ diagram referred by Graf et al. (2019) provides richer information on the below-cloud processes.

By projecting our data on the △d and △δ plot, the evaporation, equilibration, and non-exchange processes could be clearly differentiated (Fig. 4). It is apparent from Fig. 4, most of the precipitation samples are located in the fourth quadrant, indicating that evaporation is the dominant below-cloud process. A small part of samples is distributed in the first and second quadrant, and their △δ are close to 0‰ while △d are little higher than 0‰. This cluster of samples implies that the below-cloud evaporation and cloud-based isotopic fractionation tend to achieve a complete equilibrium state. Interestingly, in our samples, most of the snow samples seize the third quadrant, which is suggestive of below-cloud evaporation with less impact on them, and their initial signal after cloud-based equilibrium fractionation is well retained. According to results from numerical simulations and in-situ observations, Graf et al. (2019) summarized that raindrop size

https://doi.org/10.5194/acp-2020-312
Preprint. Discussion started: 26 May 2020

Atmospheric Chemistry and Physics
Discussions
Open Access

and precipitation intensity appear to be the important driving factors of the below-cloud processes, because raindrops with large diameter and high intensity will reduce its residence time in the atmospheric column, and lower the evaporation possibility during its way down toward the ground surface. However, as for snowfall events, it seems unreasonable to explain the strongly negative △δ from through the drop size and rain rate (Fig. 4). It is well known that snowfall events generally happen in low-temperature conditions, and corresponding to weak evaporation. Hence, rain/snow formed under such circumstances, its isotopic signals will not be largely changed by the environmental factors during its falling, which leads the △δ to be more negative with the decrease of temperature, such as the phenomenon observed in Graf's et al. (2019) study during the post-frontal periods. Our results suggest that except for drop size and rain rate, precipitation type is also an essential factor that needs to be fully considered in the below-cloud processes.

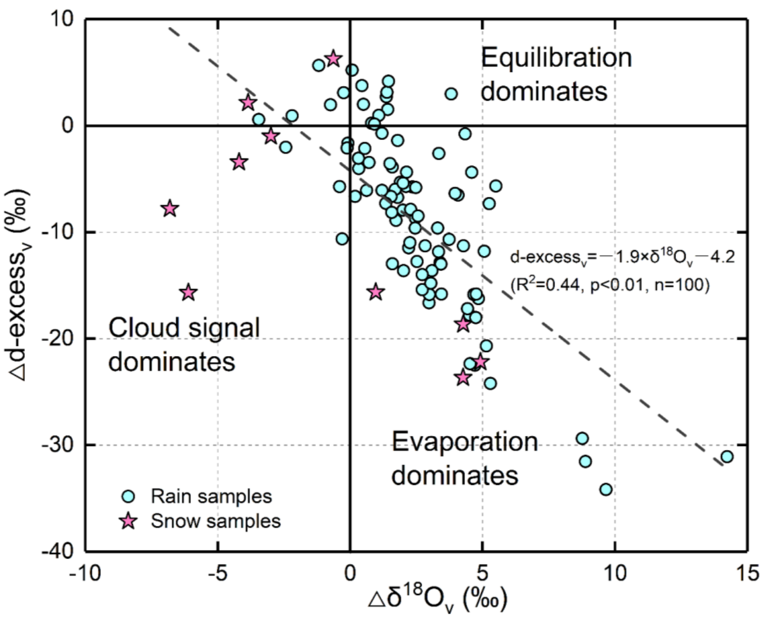

Figure 4 The projection of our data on Graf et al. (2019) suggested △d△δ-diagram. The solid lines stand for △d-excess$_v$ and △δ^{18}O$_v$ of 0‰. The dashed line corresponds to the linear fit through the samples.

Meteorological factors, such as precipitation amount, temperature, and RH, are the main factors affecting below-cloud evaporation (Li et al., 2016b; Peng et al., 2007), and have been well studied by combined with precipitation d-excess$_p$ (Ma et al., 2014; Wang et al., 2016b). In order to further analyze the below-cloud processes, we added

https://doi.org/10.5194/acp-2020-312
Preprint. Discussion started: 26 May 2020

the meteorological and isotopic information on the $\triangle d \triangle \delta$-diagram (Fig. 5). Generally, with regard to high $\triangle^{18}O_v$ samples, the corresponding meteorological condition is high temperature, low precipitation amount, and low RH (Fig. 5a-c). In contrast, under a condition of low air temperature, high RH, and large precipitation amount, the $\triangle^{18}O_v$ of samples are relatively more negative (Fig. 5a-c). As below-cloud processes are controlled by multi-variable factors, it is hard to only use one physical variable to explain the below-cloud evaporation (Ma et al., 2014; Wang et al., 2016b). For example, under the highest temperature condition (two most red dots in Fig. 5a), the below-cloud evaporation effect should be higher, and cause $\triangle^{18}O_v$ to be more positive and $\triangle$d-excess$_v$ to be more negative. However, under such circumstances, both the $\triangle^{18}O_v$ and $\triangle$d-excess$_v$ of the two samples are close to 0‰. By considering the precipitation amount, the two samples collected under the highest temperature condition are associate with a relatively larger precipitation amount which will temper the intensity of below-cloud evaporation. Similarly, the samples with lower precipitation amount is associate with high RH, and cause the $\triangle^{18}O_v$ distributed around 3‰. For the snow samples, the data with positive $\triangle^{18}O_v$ is regarding to the very low RH (Fig. 5c).

https://doi.org/10.5194/acp-2020-312
Preprint. Discussion started: 26 May 2020

Atmospheric Chemistry and Physics
Discussions

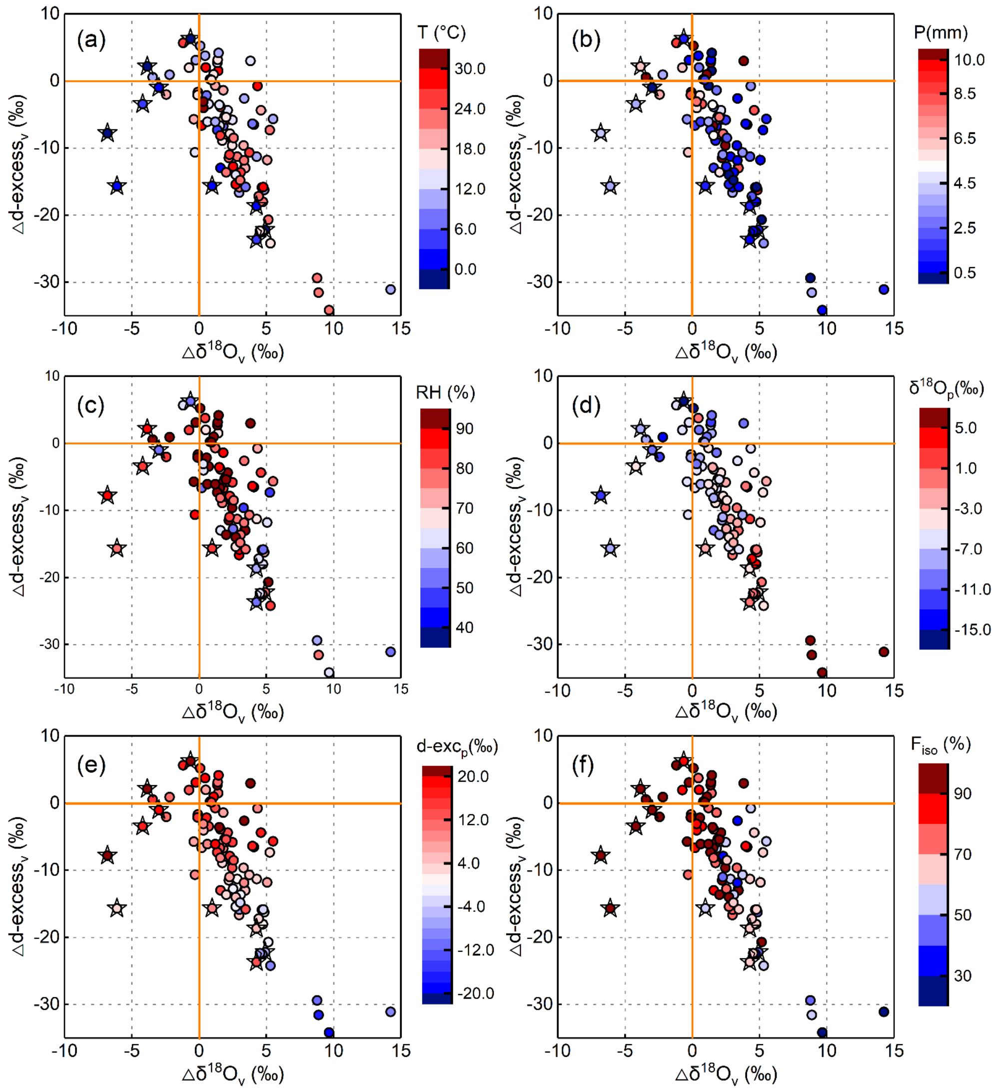

Figure 5 △d△δ-diagram for the precipitation samples with meteorological factors and precipitation isotopic information. Temperature (a); Precipitation amount (b); Relative humidity (c); $\delta^{18}O_p$ of precipitation (d); d-$excess_p$ of precipitation (e); Remaining fraction of evaporation (f). The dots with a star represent the snow samples.

In contrast to meteorological factors, the pattern of precipitation isotopic composition distribution on the △d△δ-diagram is more clear. Under the high below-cloud evaporation condition, the $\delta^{18}O_p$ is more positive and d-$excess_p$ is relatively negative (Fig. 5d and 5e). Correspondingly, the differences between equilibrated $\delta^{18}O_{eq\text{-}v}$, d-$excess_{eq\text{-}v}$ and observed $\delta^{18}O_{gr\text{-}v}$, d-$excess_{gr\text{-}v}$ are larger. Conversely, under low below-

https://doi.org/10.5194/acp-2020-312
Preprint. Discussion started: 26 May 2020

cloud evaporation conditions, mainly corresponding to the most snow samples, we could see the lowest $\delta^{18}O_p$ and highest d-excess$_p$ samples, respectively (Fig. 5d and 5e). Moreover, the $\triangle^{18}O_v$ is lower than 0‰ and $\triangle$d-excess$_v$ is placed around 0‰. Basically, the $\triangle d \triangle \delta$-diagram follows the traditional explanation, and provides more information, such as the cloud signals, equilibrium conditions, to the falling raindrops.

By contrast, the slope of the regression line of $\triangle d/\triangle \delta$ is −1.9 in our study (Fig. 4), which is more negative than result shown by Graf's et al. (2019). According to the sensitivity test by Graf et al. (2019), RH has a considerable impact on the slope of $\triangle d/\triangle \delta$. As our sampling site is located in a semi-arid area and Graf's et al. (2019) location is in the zone of a temperate marine climate, the different slope in two sites may be caused by the differences in RH. Therefore, the $\triangle d/\triangle \delta$ slope of −1.9 is possible to be related to the arid or semi-arid conditions, and $\triangle d/\triangle \delta$ slope of −0.3 could represent a general characteristic of rainfall for continental mid-latitude cold front passages. Certainly, to explore the relationship between the slope of $\triangle d/\triangle \delta$ and the climatic characteristic, more validation works need to be done in the future studies.

3.3 Comparing and analyzing the differences between F_{iso} and $F_{raindrop}$

3.3.1 The differences and reasons

In 1975, Stewart (1975) presented a set of empirical models, which is still widely used, to evaluate the below-cloud evaporation rate of the falling raindrop. However, being limited by measuring the cloud-based isotopic composition of the raindrop, many studies turn to use mass conservation model to evaluate the evaporation rate of the raindrop during its falling (Kong et al., 2013; Li et al., 2016a; Sun et al., 2020; Wang et al., 2016b). Here, to compare their differences, we used the isotopic method and mass conservation model, respectively, to calculate the F_r after the below-cloud evaporation.

As shown in Fig. 6a, the mean of computed reaming fraction is 76.3% by the isotopic method (F_{iso}), and 65.6% by the mass conservation model ($F_{raindrop}$) based on two-year statistical results. The $F_{raindrop}$ is statistically lower than the F_{iso} depending on the independent t-test ($F=1.49$, $p<0.01$). In addition, the F_{iso} and $F_{raindrop}$ show an obvious difference, the F_{iso} and $F_{raindrop}$ deviating from 1:1 line, when the F_{iso} equals to 60%~80% (Fig. 6b). On a seasonal scale, the difference between F_{iso} and $F_{raindrop}$ in spring, summer, autumn, winter is 13.7%, 12.8%, 6.0%, and 25.0%, respectively, which is the

https://doi.org/10.5194/acp-2020-312
Preprint. Discussion started: 26 May 2020

Atmospheric Chemistry and Physics
Discussions

largest in winter, and the lowest in autumn (Fig. 7).

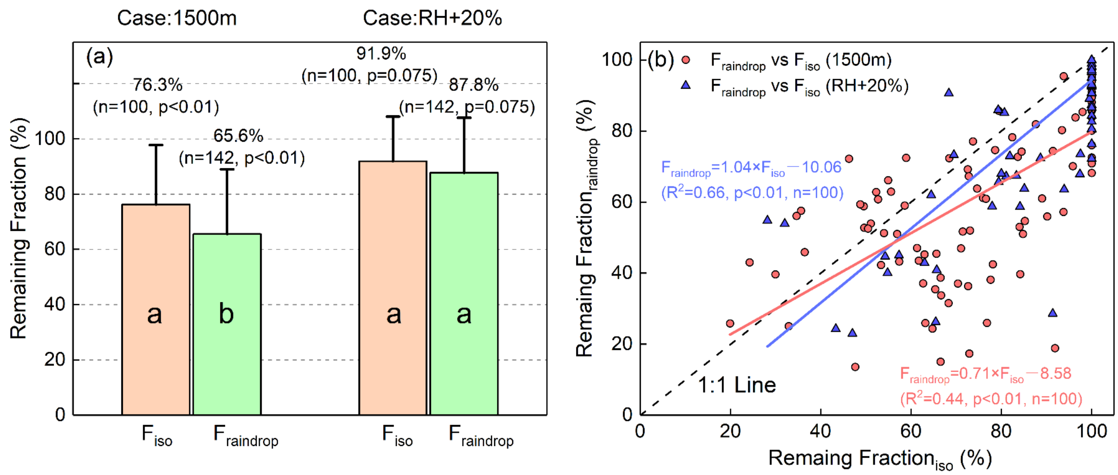

Figure 6 The comparison between the remaining fraction calculated by two methods. In (a), the taupe bars and the abbreviation of F_{iso} represent the remaining fraction calculated by the isotopic method, and the green bars and the abbreviation of $F_{raindrop}$ represent the remaining fraction calculated by the mass conservation method. Case 1500m denotes that the raindrops evaporation calculation is based on the assumption of the cloud base at 1500m, and the raindrops are formed at that altitude. Case RH+20% denotes that based on the condition of case 1500m, we calculated the remaining fraction by increasing the ground observed RH by 20%. n represents the number of samples used in statistics. The a and b in the bars denote the results of the independent t-test. In (b), the red dots represent the computed results of the remaining fraction under case 1500m condition, and the blue triangles represent the computed results under case RH+20% condition. The dash line is the 1:1 line.

https://doi.org/10.5194/acp-2020-312
Preprint. Discussion started: 26 May 2020

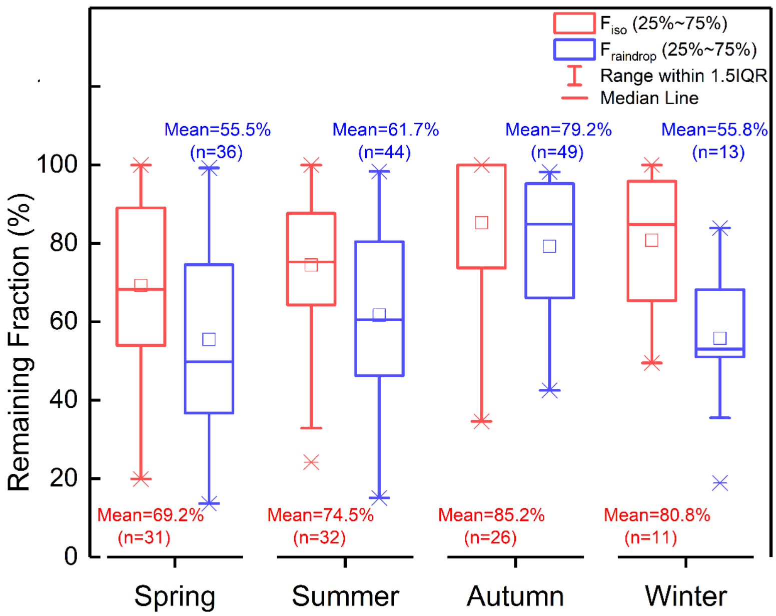

Figure 7 Comparison between the mean remaining fraction results calculated by two methods in four seasons. n represent the number of samples used in statistics.

To further explore the reason for the large differences by employing different methods, we performed the correlation analyses between meteorological factors and the remaining fraction of evaporation (Fig. S2). These analyses reveal that the most important impact factor both on F_{iso} and $F_{raindrop}$ is RH (Fig. S2b). Although precipitation amount influences F_{iso} and $F_{raindrop}$ as well, their relationship is non-linear, and its effect on F_{iso} is rather weak (R^2=0.16, Fig. S2c). For temperature, no clear correlation was found. Wang et al. (2016b) explicitly pointed that among the parameters of temperature, precipitation amount, RH, and raindrop diameter, RH generally plays a decisive role on the obtained △d-excess, which is positively correlated with the remaining fraction of raindrop.

In order to analyze the underlying reason, first, we checked the equation used to calculate F_{iso} and $F_{raindrop}$. We noted that in both methods, RH is an important parameter to compute the remaining ratio. In the equation for computing F_{iso}, the values of γ and β are highly dependent on RH. Equally, in the $F_{raindrop}$ computing equation, RH will be the decisive factor of evaporation intensity (E). Then, we tested the sensitivity between $△\delta^{18}O$ and RH under different F_{iso} levels (Fig. S3). Our results showed, under high RH condition (60%~90%), a little variation of $△\delta^{18}O$ corresponded to a wide range of F_{iso}

https://doi.org/10.5194/acp-2020-312
Preprint. Discussion started: 26 May 2020

distribution. We also noticed, under higher RH condition (above 90%), the simulated △$\delta^{18}O$ is very small, normally lower than 0.5‰. However, in reality, the △$\delta^{18}O$ is generally greater than 0.5‰. Therefore, when the actual △$\delta^{18}O$ value is larger than the theoretical value, the calculated F_{iso} results will be larger than 100%, and this is in accordance with the actual condition. Because under higher RH condition, the raindrop evaporation ratio will decrease, and in turn the F_r will appropriately increase. Moreover, in the near-saturated air column, the raindrop is hardly evaporated.

Therefore, it is reasonable to assume that when the RH is higher, the difference between the F_{iso} and $F_{raindrop}$ will be reduced. To validate our assumption, we computed the F_{iso} and $F_{raindrop}$ by increasing RH by 20%, respectively. As expected, the mean annual difference was highly reduced, and statistically there is no significant difference (Fig. 6a, independent t-test, F=5.665, p=0.075). Moreover, the F_r computed by those two methods is closer to each other, while the correlation coefficient is highly increased, and the slope is closer to 1 (Fig. 6b). For the seasonal variations of F_r, the larger differences between F_{iso} and $F_{raindrop}$ in spring and summer are regarding to the low RH in these seasons, while the small difference in autumn is related to the higher RH. For the largest difference in winter, it is most likely due to the fact that in the mass conservation model, the diameter of raindrop used to determine the terminal velocity of the raindrop (v_{end}) and the evaporation intensity (E) do not take snowfall factor into account resulting a great uncertainty in the calculation results.

3.3.2 Sensitivity test

In the below-cloud isotopic evaporation model (eq. 7), the two controlling factors are the equilibrium fractionation factor (α) and the RH. As the equilibrium fractionation factor varies with the cloud base altitude (mainly caused by the variation of temperature), we used the different altitudes to represent the variations of α. In order to assess the relevance of different ambient conditions for the raindrop evaporation, a sensitivity test of F_r under different altitude and RH scenarios is exhibited in Fig. S4. With the increase of altitude, the F_r is gradually decreased. It is well known that with the increase of altitude, the raindrop falling distance will increase, and correspondingly the falling time will be extended. As a result, more fraction of raindrops would be evaporated in the unsaturated atmospheric columns. When the RH increases by 20%, the atmospheric columns is near saturated, and largely decrease the evaporation possibility of falling raindrops. Conversely, the decrease of RH will strongly increase the evaporation proportion of falling raindrops. In addition, according to Fig. S4, the F_r

https://doi.org/10.5194/acp-2020-312
Preprint. Discussion started: 26 May 2020

seems to be more sensitive to the changing of RH than that of altitude.

Overall, in our study, the mass conservation method will overestimate the raindrop evaporation ratios relative to the isotopic method. The overestimation may be related to the low RH in our studying location. If we increase the RH by 20%, there is no significant difference between the two methods. This indicates that in high RH areas, either method could be used to calculate the F_r. However, in those arid and semi-arid areas, where the RH is relatively low, and the high latitude regions, where snowfall is frequent in winter, we need to cautiously use the result computed by the mass conservation method. In the future, it will be promising to study the raindrop formation height and upper atmospheric water vapor isotopic composition when considering the below-cloud processes of raindrop.

3.4 The characteristics of below-cloud evaporation of raindrop in Xi'an

As the phenomenon of below-cloud evaporation is very common in arid and semi-arid regions, to explore the information contained in the precipitation isotopic composition, it is important to clearly know that how much of the raindrops have been evaporated before they land on the ground. Here, we summarized the seasonal variations of F_{iso} in Xi'an (Fig. 8).

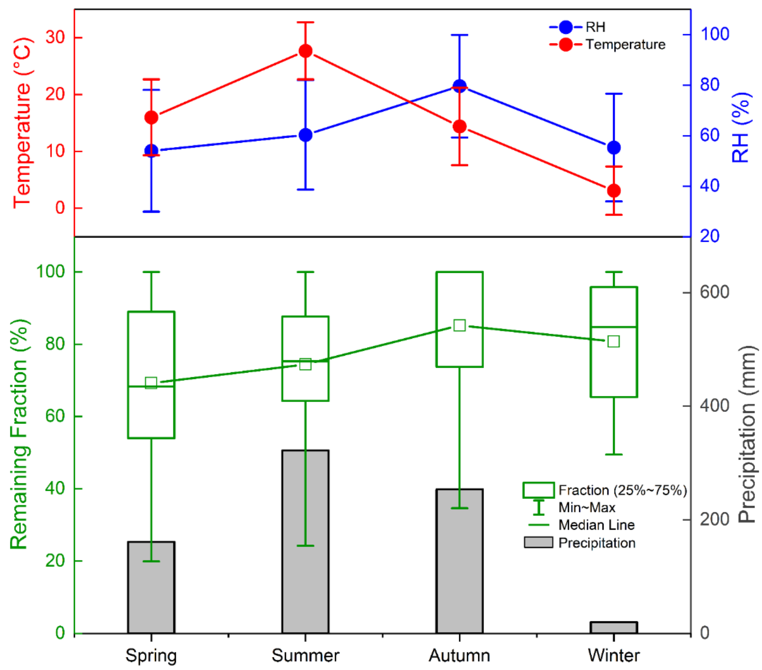

https://doi.org/10.5194/acp-2020-312
Preprint. Discussion started: 26 May 2020

Figure 8 The variations of temperature, relative humidity, precipitation amount and mean remaining fraction of evaporated raindrops in four seasons in Xi'an

By seasonally dividing the precipitation isotopic composition on the △d△δ-diagram, it showed that samples collected in spring and summer dominate the evaporation phase, reflecting a stronger evaporation influence, while most of the winter precipitation and part of autumn precipitation monopolize the cloud signal phase indicating a weak or no below-cloud evaporation on these samples (Fig. S5). In addition, part of the autumn samples, in which the below-cloud evaporation and cloud-based isotopic exchange tends to achieve a complete equilibrium state is distributed in the equilibration phase (Fig. S5). Moreover, the raindrops F_{iso} distribution on the △d△δ-diagram is also related to the below-cloud processes (Fig. 5f).

The mean raindrop evaporation rate is highest in spring and lowest in autumn based on two-year data (Fig. 8). The seasonal variation of F_{iso} basically followed the trend of seasonal variation of RH. Although the precipitation amount is highest in the summer, the temperature is extremely high and RH is relatively low, which causes the high evaporation rate in summer. In winter, the low evaporation rate may be related to the precipitation type, because snowfall is the main deposition type in this season.

4 Conclusions

The below-cloud processes acting on precipitation are complex and changeable, especially in the arid and semi-arid regions. Previously, using the slope of LMWL and d-excess of precipitation, we can only speculate the raindrops experienced below-cloud processes according to the relative change of precipitation isotopic composition. However, to display our data on the △d△δ-diagram, which is suggested by Graf et al. (2019), we can more intuitively determine the happened below-cloud processes on the falling raindrops. The △d△δ-diagram provides a new tool for us to qualitatively realize the below-cloud processes of raindrops.

In this study, based on the two-year precipitation data collected in Xi'an, we systematically analyze its below-cloud processes, and get the following main conclusions:

1. In Xi'an, the precipitation isotopic signals mainly record the information of water vapor isotopic composition, but the signals could be altered by the below-cloud evaporation effect. This remind us to be cautious to study the hydrological cycle and

https://doi.org/10.5194/acp-2020-312
Preprint. Discussion started: 26 May 2020

Atmospheric Chemistry and Physics Discussions

climate changes by using precipitation isotopic signals in the arid and semi-arid regions.
2. Our work validates the general applicability of the △d△δ-diagram. According to △d△δ-diagram, the below-cloud evaporation is the main process during the raindrops falling. For the snowfall samples, they are less influenced by the below-cloud processes, and preserve its initial water vapor information. Hence, our results further strengthen the reliability by using ice-core to reconstruct the paleoclimate, paleoenvironment, and paleohydrology in the cold area. The different △d/△δ slopes in our work and Graf's et al. (2019) study may represent the different climate conditions, and it will be more convincible to explore the slope for more climatic regions in future studies.
3. Compared with the isotopic method, the evaporation rate computed by the mass conservation model is overestimated. Relative humidity is the main controlling factor in computing the remaining fraction of raindrops below-cloud evaporation. Due to more undeterminable parameters in the mass conservation model, such as raindrop diameter, evaporation intensity, raindrop falling velocity, and no consideration of precipitation type, it is more suitable to use isotopic model to calculate the remaining fraction of evaporated raindrops.
4. In the semi-arid city of CLP, the evaporation rates are higher in spring and summer, and lower in autumn and winter, and this is related to the variation of local RH.

Data availability

The datasets can be obtained from the TableS1.

Author contribution

Meng Xing and Weiguo Liu designed the experiments, interpreted the results, and prepared the manuscript with contributions from all co-authors. Meng Xing and Jing Hu analyzed the precipitation and water vapor samples. Jing Hu maintained the experimental instruments.

Competing interests

The authors declare that they have no conflict of interest.

Acknowledgment

This work was supported by China haze formation mechanism research (SKLLQGZD1701), National Research Program for Key Issues in Air Pollution Control (DQGG0105-02), Science Foundation of China (No. 41303011), and China scholarship council. The authors would like to thank Mr. Xijing Cao for helping to collect precipitation samples.

References

Aemisegger, F., Sturm, P., Graf, P., Sodemann, H., Pfahl, S., Knohl, A. and Wernli, H.: Measuring variations of δ 18O and δ 2H in atmospheric water vapour using two commercial laser-based spectrometers: An instrument characterisation study, Atmos. Meas. Tech., 5(7), 1491–1511, doi:10.5194/amt-5-1491-2012, 2012.

Aemisegger, F., Spiegel, J. K., Pfahl, S., Sodemann, H., Eugster, W. and Wernli, H.: Isotope meteorology of cold front passages: A case study combining observations and modeling, Geophys. Res. Lett., 42(13), 5652–5660, doi:10.1002/2015GL063988, 2015.

Bastrikov, V., Steen-Larsen, H. C., Masson-Delmotte, V., Gribanov, K., Cattani, O., Jouzel, J. and Zakharov, V.: Continuous measurements of atmospheric water vapour isotopes in western Siberia (Kourovka), Atmos. Meas. Tech., 7(6), 1763–1776, doi:10.5194/amt-7-1763-2014, 2014.

Benetti, M., Reverdin, G., Pierre, C., Merlivat, L., Risi, C., Steen-Larsen, H. C. and Vimeux, F.: Deuterium excess in marine water vapor: Dependency on relative humidity and surface wind speed during evaporation, J. Geophys. Res., 119(2), 584–593, doi:10.1002/2013JD020535, 2014.

Bowen, G. J., Cai, Z., Fiorella, R. P. and Putman, A. L.: Isotopes in the Water Cycle: Regional- to Global-Scale Patterns and Applications, Annu. Rev. Earth Planet. Sci., 47(1), 453–479, doi:10.1146/annurev-earth-053018-060220, 2019.

Cai, Y., Cheng, H., An, Z., Edwards, R. L., Wang, X., Tan, L. and Wang, J.: Large variations of oxygen isotopes in precipitation over south-central Tibet during Marine Isotope Stage 5, Geology, 38(3), 243–246, doi:10.1130/G30306.1, 2010.

Chakraborty, S., Sinha, N., Chattopadhyay, R., Sengupta, S., Mohan, P. M. and Datye, A.: Atmospheric controls on the precipitation isotopes over the Andaman Islands, Bay of Bengal, Sci. Rep., 6, 19555 [online] Available from: https://doi.org/10.1038/srep19555, 2016.

Christner, E., Aemisegger, F., Pfahl, S., Werner, M., Cauquoin, A., Schneider, M., Hase, F., Barthlott, S. and Schädler, G.: The Climatological Impacts of Continental Surface Evaporation, Rainout, and Subcloud Processes on δD of Water Vapor and Precipitation in Europe, J. Geophys. Res. Atmos., 123(8), 4390–4409, doi:10.1002/2017JD027260, 2018.

Clark, I. D. and Fritz, P.: Environmental Isotopes in Hydrogeology, Lewis, Boca Raton, Florida., 1997.

Craig, H.: Isotopic Variations in Meteoric Waters, Science (80-.)., 133(3465), 1702–1703, 1961.

Crosson, E. R.: A cavity ring-down analyzer for measuring atmospheric levels of methane, carbon dioxide, and water vapor, Appl. Phys. B, 92(3), 403–408, doi:10.1007/s00340-008-3135-y, 2008.

Dansgaard, W.: Stable isotopes in precipitation, Tellus, 16(4), 436–468, doi:10.3402/tellusa.v16i4.8993, 1964.

Deshpande, R. D., Maurya, A. S., Kumar, B., Sarkar, A. and Gupta, S. K.: Rain-vapor interaction and vapor source identification using stable isotopes from semiarid western India, J. Geophys. Res. Atmos., 115(23), 1–11, doi:10.1029/2010JD014458, 2010.

Ellehoj, M. D., Steen-Larsen, H. C., Johnsen, S. J. and Madsen, M. B.: Ice-vapor equilibrium fractionation factor of hydrogen and oxygen isotopes: experimental investigations and implications for stable water isotope studies, Rapid Commun. Mass Spectrom. Rcm, 27(19), 2149–2158, 2013.

Fiorella, R. P., Bares, R., Lin, J. C., Ehleringer, J. R. and Bowen, G. J.: Detection and variability of combustion-derived vapor in an urban basin, Atmos. Chem. Phys., 18(12), 8529–8547, doi:10.5194/acp-18-8529-2018, 2018.

Froehlich, K., Kralik, M., Papesch, W., Rank, D., Scheifinger, H. and Stichler, W.: Deuterium excess in precipitation of Alpine regions – moisture recycling, Isotopes Environ. Health Stud., 44(1), 61–70, doi:10.1080/10256010801887208, 2008.

Gat, J. R.: OXYGEN AND HYDROGEN ISOTOPES IN THE HYDROLOGIC CYCLE, Annu. Rev. Earth Planet. Sci., 24(1), 225–262, doi:10.1146/annurev.earth.24.1.225, 1996.

Gorski, G., Strong, C., Good, S. P., Bares, R., Ehleringer, J. R. and Bowen, G. J.: Vapor hydrogen and oxygen isotopes reflect water of combustion in the urban atmosphere, Proc. Natl. Acad. Sci., 112(11), 3247–3252, doi:10.1073/pnas.1424728112, 2015.

Graf, P., Wernli, H., Pfahl, S. and Sodemann, H.: A new interpretative framework for below-cloud effects on stable water isotopes in vapour and rain, Atmos. Chem. Phys., 19(2), 747–765, doi:10.5194/acp-19-747-2019, 2019.

Griffis, T. J., Wood, J. D., Baker, J. M., Lee, X., Xiao, K., Chen, Z., Welp, L. R., Schultz, N. M., Gorski, G., Chen, M. and Nieber, J.: Investigating the source, transport, and isotope composition of water vapor in the planetary boundary layer, Atmos. Chem. Phys., 16(8), 5139–5157, doi:10.5194/acp-16-5139-2016, 2016.

Gupta, P., Noone, D., Galewsky, J., Sweeney, C. and Vaughn, B. H.: Demonstration of high-precision continuous measurements of water vapor isotopologues in laboratory and remote field deployments using wavelength-scanned cavity ring-down spectroscopy (WS-CRDS) technology, Rapid Commun Mass Spectrom, 23(16), 2009.

Horita, J. and Wesolowski, D. J.: Liquid-vapor fractionation of oxygen and hydrogen isotopes of water from the freezing to the critical temperature, Geochim. Cosmochim. Acta, 58(16), 3425–3437, 1994.

Jacob, H. and Sonntag, C.: An 8-year record of the seasonal variation of 2 H and 18 O in atmospheric water vapour and precipitation at Heidelberg, Germany, Tellus B Chem. Phys.

https://doi.org/10.5194/acp-2020-312
Preprint. Discussion started: 26 May 2020

Meteorol., 43(3), 291–300, doi:10.3402/tellusb.v43i3.15276, 1991.

Jeelani, G., Deshpande, R. D., Galkowski, M. and Rozanski, K.: Isotopic composition of daily precipitation along the southern foothills of the Himalayas: Impact of marine and continental sources of atmospheric moisture, Atmos. Chem. Phys., 18(12), 8789–8805, doi:10.5194/acp-18-8789-2018, 2018.

Kong, Y., Pang, Z. and Froehlich, K.: Quantifying recycled moisture fraction in precipitation of an arid region using deuterium excess . Tellus Series B Chem Phys Meteorol Quantifying recycled moisture fraction in precipitation of an arid region using deuterium excess, Tellus B, 65(August 2015), 1–8, doi:10.3402/tellusb.v65i0.19251, 2013.

Laskar, A. H., Huang, J. C., Hsu, S. C., Bhattacharya, S. K., Wang, C. H. and Liang, M. C.: Stable isotopic composition of near surface atmospheric water vapor and rain-vapor interaction in Taipei, Taiwan, J. Hydrol., 519(PB), 2091–2100, doi:10.1016/j.jhydrol.2014.10.017, 2014.

Li, L. and Garzione, C. N.: Spatial distribution and controlling factors of stable isotopes in meteoric waters on the Tibetan Plateau : Implications for paleoelevation reconstruction, Earth Planet. Sci. Lett., 460, 302–314, doi:10.1016/j.epsl.2016.11.046, 2017.

Li, Z., Qi, F., Wang, Q. J., Kong, Y., Cheng, A., Song, Y., Li, Y., Li, J. and Guo, X.: Contributions of local terrestrial evaporation and transpiration to precipitation using δ 18 O and D-excess as a proxy in Shiyang inland river basin in China, Glob. Planet. Chang., 146, 140–151, 2016a.

Li, Z., Feng, Q., Wang, Y., Li, J., Guo, X. and Li, Y.: Effect of sub-cloud evaporation on the δ 18 O of precipitation in Qilian Mountains and Hexi Corridor , China, Sci. Cold Arid Reg., 8(5), 378–387, doi:10.3724/SP.J.1226.2016.00378.Effect, 2016b.

Liu, W., Feng, X., Liu, Y., Zhang, Q. and An, Z.: δ18O values of tree rings as a proxy of monsoon precipitation in arid Northwest China, Chem. Geol., 206(1), 73–80, doi:https://doi.org/10.1016/j.chemgeo.2004.01.010, 2004.

Liu, W., Liu, H., Wang, Z., An, Z. and Cao, Y.: Hydrogen isotopic compositions of long-chain leaf wax n-alkanes in Lake Qinghai sediments record palaeohydrological variations during the past 12 ka, Quat. Int., 449, 67–74, doi:https://doi.org/10.1016/j.quaint.2017.05.024, 2017a.

Liu, W., Wang, H., Leng, Q., Liu, H., Zhang, H. and Xing, M.: Hydrogen isotopic compositions along a precipitation gradient of Chinese Loess Plateau : Critical roles of precipitation / evaporation and vegetation change as controls for leaf wax δ D, Chem. Geol., 528(April), 119278, doi:10.1016/j.chemgeo.2019.119278, 2019.

Liu, Y., Liu, H., Song, H., Li, Q., Burr, G. S., Wang, L. and Hu, S.: A monsoon-related 174-year relative humidity record from tree-ring δ18O in the Yaoshan region, eastern central China, Sci. Total Environ., 593–594, 523–534, doi:https://doi.org/10.1016/j.scitotenv.2017.03.198, 2017b.

Ma, Q., Zhang, M., Wang, S., Wang, Q., Liu, W., Li, F. and Chen, F.: An investigation of moisture sources and secondary evaporation in Lanzhou, Northwest China, Environ. Earth Sci., 71(8), 3375–3385, doi:10.1007/s12665-013-2728-x, 2014.

Müller, S., Stumpp, C., Sørensen, J. H. and Jessen, S.: Spatiotemporal variation of stable isotopic composition in precipitation: Post-condensational effects in a humid area, Hydrol. Process., 31(18), 3146–3159, doi:10.1002/hyp.11186, 2017.

https://doi.org/10.5194/acp-2020-312
Preprint. Discussion started: 26 May 2020

Noone, D., Galewsky, J., Sharp, Z. D., Worden, J., Barnes, J., Baer, D., Bailey, A., Brown, D. P., Christensen, L., Crosson, E., Dong, F., Hurley, J. V., Johnson, L. R., Strong, M., Toohey, D., Van Pelt, A. and Wright, J. S.: Properties of air mass mixing and humidity in the subtropics from measurements of the D/H isotope ratio of water vapor at the Mauna Loa Observatory, J. Geophys. Res. Atmos., 116(22), 1–18, doi:10.1029/2011JD015773, 2011.

Noone, D., Risi, C., Bailey, A., Berkelhammer, M., Brown, D. P., Buenning, N., Gregory, S., Nusbaumer, J., Schneider, D., Sykes, J., Vanderwende, B., Wong, J., Meillier, Y. and Wolfe, D.: Determining water sources in the boundary layer from tall tower profiles of water vapor and surface water isotope ratios after a snowstorm in Colorado, Atmos. Chem. Phys., 13(3), 1607–1623, doi:10.5194/acp-13-1607-2013, 2013.

Peng, H., Mayer, B., Harris, S. and Krouse, H. R.: The influence of below-cloud secondary effects on the stable isotope composition of hydrogen and oxygen in precipitation at Calgary, Alberta, Canada, Tellus, Ser. B Chem. Phys. Meteorol., 59(4), 698–704, doi:10.1111/j.1600-0889.2007.00291.x, 2007.

Peng, T. R., Liu, K. K., Wang, C. H. and Chuang, K. H.: A water isotope approach to assessing moisture recycling in the island-based precipitation of Taiwan: A case study in the western Pacific, Water Resour. Res., 47(8), 1–11, doi:10.1029/2010WR009890, 2011.

Putman, A. L., Fiorella, R. P., Bowen, G. J. and Cai, Z.: A Global Perspective on Local Meteoric Water Lines: Meta-analytic Insight into Fundamental Controls and Practical Constraints, Water Resour. Res., 2019WR025181, doi:10.1029/2019WR025181, 2019.

Rangarajan, R., Laskar, A. H., Bhattacharya, S. K., Shen, C. C. and Liang, M. C.: An insight into the western Pacific wintertime moisture sources using dual water vapor isotopes, J. Hydrol., 547, 111–123, doi:10.1016/j.jhydrol.2017.01.047, 2017.

Salamalikis, V., Argiriou, A. A. and Dotsika, E.: Isotopic modeling of the sub-cloud evaporation effect in precipitation, Sci. Total Environ., 544, 1059–1072, doi:10.1016/j.scitotenv.2015.11.072, 2016.

Salmon, O. E., Welp, L. R., Baldwin, M., Hajny, K., Stirm, B. H. and Shepson, P. B.: Vertical profile observations of water vapor deuterium excess in the lower troposphere, Atmos. Chem. Phys. Discuss., (January), 1–35, doi:10.5194/acp-2018-1313, 2019.

Steen-Larsen, H. C., Johnsen, S. J., Masson-Delmotte, V., Stenni, B., Risi, C., Sodemann, H., Balslev-Clausen, D., Blunier, T., Dahl-Jensen, D., Ellehøj, M. D., Falourd, S., Grindsted, A., Gkinis, V., Jouzel, J., Popp, T., Sheldon, S., Simonsen, S. B., Sjolte, J., Steffensen, J. P., Sperlich, P., Sveinbjörnsdóttir, A. E., Vinther, B. M. and White, J. W. C.: Continuous monitoring of summer surface water vapor isotopic composition above the Greenland Ice Sheet, Atmos. Chem. Phys., 13(9), 4815–4828, doi:10.5194/acp-13-4815-2013, 2013.

Steen-Larsen, H. C., Masson-Delmotte, V., Hirabayashi, M., Winkler, R., Satow, K., Prié, F., Bayou, N., Brun, E., Cuffey, K. M., Dahl-Jensen, D., Dumont, M., Guillevic, M., Kipfstuhl, S., Landais, A., Popp, T., Risi, C., Steffen, K., Stenni, B. and Sveinbjörnsdottír, A. E.: What controls the isotopic composition of Greenland surface snow?, Clim. Past, 10(1), 377–392, doi:10.5194/cp-10-377-2014, 2014.

Stewart, M. K.: Stable isotope fractionation due to evaporation and isotopic exchange of falling waterdrops: Applications to atmospheric processes and evaporation of lakes, J. Geophys. Res., 80(9), 1133–1146, doi:10.1029/JC080i009p01133, 1975.

Sun, C., Chen, Y., Li, J., Chen, W. and Li, X.: Stable isotope variations in precipitation in the northwesternmost Tibetan Plateau related to various meteorological controlling factors, Atmos. Res., 227(April), 66–78, doi:10.1016/j.atmosres.2019.04.026, 2019.

Sun, C., Chen, W., Chen, Y. and Cai, Z.: Stable isotopes of atmospheric precipitation and its environmental drivers in the Eastern Chinese Loess Plateau , China, J. Hydrol., 581(November 2019), 124404, doi:10.1016/j.jhydrol.2019.124404, 2020.

Tan, L., An, Z., Huh, C.-A., Cai, Y., Shen, C.-C., Shiau, L.-J., Yan, L., Cheng, H. and Edwards, R. L.: Cyclic precipitation variation on the western Loess Plateau of China during the past four centuries, Sci. Rep., 4(1), 6381, doi:10.1038/srep06381, 2014.

Thompson, L. G., Yao, T., Mosley-Thompson, E., Davis, M. E., Henderson, K. A. and Lin, P.-N.: A High-Resolution Millennial Record of the South Asian Monsoon from Himalayan Ice Cores, Science (80-.)., 289(5486), 1916 LP – 1919, doi:10.1126/science.289.5486.1916, 2000.

Tian, C., Wang, L., Kaseke, K. F. and Bird, B. W.: Stable isotope compositions (δ 2 H , δ 18 O and δ 17 O) of rainfall and snowfall in the central United States, Sci. Rep., (October 2017), 1–15, doi:10.1038/s41598-018-25102-7, 2018.

Wan, H., Liu, W. and Xing, M.: Isotopic composition of atmospheric precipitation and its tracing significance in the Laohequ Basin, Loess plateau, China, Sci. Total Environ., 640–641(May), 989–996, doi:10.1016/j.scitotenv.2018.05.338, 2018.

Wang, S., Zhang, M., Che, Y., Chen, F. and Fang, Q.: Contribution of recycled moisture to precipitation in oases of arid central Asia: A stable isotope approach, Water Resour. Res., 52(4), 3246–3257, doi:10.1002/2015WR018135, 2016a.

Wang, S., Zhang, M., Che, Y., Zhu, X. and Liu, X.: Influence of Below-Cloud Evaporation on Deuterium Excess in Precipitation of Arid Central Asia and Its Meteorological Controls, J. Hydrometeorol., 17(7), 1973–1984, doi:10.1175/JHM-D-15-0203.1, 2016b.

Wang, S., Zhang, M., Hughes, C. E., Crawford, J., Wang, G., Chen, F., Du, M., Qiu, X. and Zhou, S.: Meteoric water lines in arid Central Asia using event-based and monthly data, J. Hydrol., 562(May), 435–445, doi:10.1016/j.jhydrol.2018.05.034, 2018a.

Wang, Z., An, Z., Liu, Z., Qiang, X., Zhang, F. and Liu, W.: Hydroclimatic variability in loess δDwax records from the central Chinese Loess Plateau over the past 250 ka, J. Asian Earth Sci., 155, 49–57, doi:https://doi.org/10.1016/j.jseaes.2017.11.008, 2018b.

Welp, L. R., Lee, X., Kim, K., Griffis, T. J., Billmark, K. A. and Baker, J. M.: δ18O of water vapour, evapotranspiration and the sites of leaf water evaporation in a soybean canopy, Plant, Cell Environ., 31(9), 1214–1228, doi:10.1111/j.1365-3040.2008.01826.x, 2008.

Welp, L. R., Lee, X., Griffis, T. J., Wen, X. F., Xiao, W., Li, S., Sun, X., Hu, Z., Val Martin, M. and Huang, J.: A meta-analysis of water vapor deuterium-excess in the midlatitude atmospheric surface layer, Global Biogeochem. Cycles, 26(3), 1–12, doi:10.1029/2011GB004246, 2012.

Wen, X., Yang, B., Sun, X. and Lee, X.: Evapotranspiration partitioning through in-situ oxygen isotope measurements in an oasis cropland, Agric. For. Meteorol., 230–231, 89–96, doi:10.1016/j.agrformet.2015.12.003, 2016.

Wen, X. F., Zhang, S. C., Sun, X. M., Yu, G. R. and Lee, X.: Water vapor and precipitation isotope ratios in Beijing, China, J. Geophys. Res. Atmos., 115(1), 1–10, doi:10.1029/2009JD012408, 2010.

Yao, T., Thompson, L. G., Mosley-Thompson, E., Zhihong, Y., Xingping, Z. and Lin, P.-N.: Climatological significance of δ18O in north Tibetan ice cores, J. Geophys. Res. Atmos., 101(D23), 29531–29537, doi:10.1029/96JD02683, 1996.

Yao, T., Masson-Delmotte, V., Gao, J., Yu, W., Yang, X., Risi, C., Sturm, C., Werner, M., Zhao, H., He, Y., Ren, W., Tian, L., Shi, C. and Hou, S.: A review of climatic controls on δ18O in precipitation over the Tibetan Plateau: Observations and simulations, Rev. Geophys., 51(4), 525–548, doi:10.1002/rog.20023, 2013.

Yu, W., Tian, L., Ma, Y., Xu, B. and Qu, D.: Simultaneous monitoring of stable oxygen isotope composition in water vapour and precipitation over the central Tibetan Plateau, Atmos. Chem. Phys., 15(18), 10251–10262, doi:10.5194/acp-15-10251-2015, 2015.

Yu, W., Tian, L., Risi, C., Yao, T., Ma, Y., Zhao, H., Zhu, H., He, Y., Xu, B., Zhang, H. and Qu, D.: δ18O records in water vapor and an ice core from the eastern Pamir Plateau: Implications for paleoclimate reconstructions, Earth Planet. Sci. Lett., 456, 146–156, doi:10.1016/j.epsl.2016.10.001, 2016.

Zhang, M. and Wang, S.: A review of precipitation isotope studies in China: Basic pattern and hydrological process, J. Geogr. Sci., 26(7), 921–938 [online] Available from: http://www.geogsci.com, 2016.

Zhao, L., Liu, X., Wang, N., Kong, Y., Song, Y., He, Z., Liu, Q. and Wang, L.: Contribution of recycled moisture to local precipitation in the inland Heihe River Basin, Agric. For. Meteorol., 271(July 2018), 316–335, doi:10.1016/j.agrformet.2019.03.014, 2019.

Zhu, G. F., Li, J. F., Shi, P. J., He, Y. Q., Cai, A., Tong, H. L., Liu, Y. F. and Yang, L.: Relationship between sub-cloud secondary evaporation and stable isotope in precipitation in different regions of China, Environ. Earth Sci., 75(10), 876, 2016.